







Evaluating the suitability of different terrains for sustaining human settlements according to the local elevation range in China using the ASTER GDEM

XIAO Chi-wei  <http://orcid.org/0000-0003-3477-9406>; e-mail: xiaocw@igsnr.ac.cn

FENG Zhi-ming  <http://orcid.org/0000-0002-3682-4955>; e-mail: fengzm@igsnr.ac.cn

LI Peng*  <http://orcid.org/0000-0002-0849-5955>;  e-mail: lip@igsnr.ac.cn

YOU Zhen  <http://orcid.org/0000-0001-8477-5142>; e-mail: youz@igsnr.ac.cn

TENG Jia-kun  <http://orcid.org/0000-0001-9207-3765>; e-mail: jiakunteng@163.com

*Corresponding author

Institute of Geographic Sciences and Natural Resources Research, Chinese Academy of Sciences, Beijing 100101, China

College of Resources and Environment, University of Chinese Academy of Sciences, Beijing 100049, China

Citation: Xiao CW, Feng ZM, Li P, et al. (2018) Evaluating the suitability of different terrains for sustaining human settlements according to the local elevation range in China using the ASTER GDEM. *Journal of Mountain Science* 15(12). <https://doi.org/10.1007/s11629-018-5058-3>

© Science Press, Institute of Mountain Hazards and Environment, CAS and Springer-Verlag GmbH Germany, part of Springer Nature 2018

Abstract: The topographical suitability assessment of human settlements (SAHS) creates a solid foundation for regional population distribution and socio-economic development. Local elevation range (LER) is an important factor that can be used to assess the suitability of different terrains for sustaining human settlements. However, current digital elevation model (DEM)-based LER products suffer from some challenges typically because of their subjectively selected neighborhood scales and coarser spatial resolution. In this study, we initially determined the optimal statistical window and then calculated the appropriate LER with the finer resolution data of the Advanced Spaceborne Thermal Emission and Reflection Radiometer Global DEM (ASTER GDEM) products for China. Then, the appropriate LER was used to evaluate the topographical SAHS and its correlations with the

national gridded population distribution (1 km × 1 km) in 2010. The results show that the optimal statistical window for calculating a 1 arc-second (about 30 m) resolution GDEM LER for China can be determined using a 51 × 51 grid unit (width × height) within a rectangular neighborhood, corresponding to an area of about 2.34 km². Secondly, the LER values in the southern and western China were greater than those of the north and east, showing a trend which consistently reflects the general spatial features of landforms. Finally, the relationship between GDEM LER and population density was highly correlated with the R^2 value of 0.81. It showed that 85.22% of the Chinese population was located in areas where the LER is lower than 500 m. The topographically suitable area within China decreased from the southeastern coastal zone towards the northwestern inland areas due to transition from plains and basins to plateaus and mountains. The total area of moderate to high suitable level was 423.84×10^4 km², or 44.15% of the total land area, with 88.17% of the national population. Our study demonstrates the usefulness of appropriate LER in evaluating the topographical

Received: 31 May 2018

1st Revision: 13 June 2018

2nd Revision: 26 August 2018

Accepted: 12 November 2018

SAHS as well as its significant impact on population distribution.

Keywords: Human settlements; Topographical suitability; Local elevation range (LER); Advanced Spaceborne Thermal Emission and Reflection Radiometer Global DEM (ASTER GDEM); China

Introduction

Although research on human settlements has gradually developed since this concept firstly coined by Constantinos A. Doxiadis in the 1950s (Doxiadis 1975), no unified definition of this terminology has yet been presented (Wang et al. 2017). The concept of human settlements is interdisciplinary and aims to examine the relationship between population distribution and natural environments by measuring the degree of natural suitability (Wu 2001). Thus, human settlements have become the focus of numerous fields, including population geography (Tritsch and Le Tourneau 2016), climatic change (Zhang et al. 2005), residential environments (Esch et al. 2014), urban planning (Emmanuel 2005), and the suitability of settlements (Richard et al. 2008). Given the development of urbanization and industrialization, human settlements have undergone dramatic environmental changes (Ma et al. 2016), such as vegetation loss (Taubenböck et al. 2012), urban heat island effects, and air pollution (Wu et al. 2013). These effects on living conditions of human settlements have garnered a great deal of worldwide attention (Chiang and Liang 2013; Kotus and Rzeszewski 2013).

A number of studies have utilized techniques of remote sensing and geographic information systems to evaluate the suitability assessment of human settlements (SAHS) to date (Emmanuel 2005; Feng et al. 2009, 2010; Li et al. 2011; Wei et al. 2013; Zhu et al. 2016). Indeed, the SAHS is likely to further promote regional coordinated development among population, natural resources, and environment (Ma et al. 2016; Wang et al. 2017). Human settlements are influenced by a range of natural factors, including terrain, climate, hydrology, land use, vegetation coverage and combinations thereof (Feng et al. 2009, 2010; Li et al. 2011). Currently, both single (Emmanuel 2005;

Feng et al. 2008; Tan et al. 2008) and comprehensive evaluation models (Feng et al. 2009, 2010; Li et al. 2011; Zhu et al. 2016) that address the SAHS have been widely used, especially at regional, provincial, and national scales within China (Wei et al. 2013; Yang and Zhang 2016; Wang et al. 2017). However, the suitability evaluation of different terrains for sustaining human settlements has not been fully investigated, although topography is one of the fundamental factors (Feng et al. 2009, 2010; Liu et al. 2015). Local elevation range (LER), in particular, has been used as a crucial structural parameter in the aspect of terrain suitability (Liu et al. 2015; Li and Feng 2016; Xiao et al. 2018) and its relationship with population distribution (Feng et al. 2007, 2008).

Currently, the global digital elevation model (DEM) have been widely used for applied studies on terrain relief (or LER) and landform classification (Meybeck et al. 2002; Fang and Yang 2016; Xiao et al. 2018). There are several commonly used datasets for global DEMs, including Global 30-Arc-Second Elevation data (GTOPO 30; 30 arc seconds) (USGS 1996), Shuttle Radar Topography Mission data (SRTM; 3 arc and 1 arc seconds) (Rodriguez et al. 2006), Global Multi-Resolution Terrain Elevation data 2010 (GMTED 2010; 30, 15, and 7.5 arc seconds) (USGS 2010), and Advanced Spaceborne Thermal Emission and Reflection Radiometer Global Digital Elevation Model (ASTER GDEM; 1 arc-second) data (Tachikawa et al. 2011). Due to the coarse spatial resolution of GTOPO 30 and GMTED 2010, their application demands were limited (Xiao et al. 2018). Therefore, researchers have mainly focused on the 1 arc second resolution SRTM-3 and GDEM (Podobnikar 2012; Zhong and Liu 2014; Satgé et al. 2015; Yue et al. 2017). However, the inaccurate void filling of SRTM data (Yang et al. 2011) and lack of coverage at higher latitudes (Yang et al. 2011; Yue et al. 2017) are insufficient in dealing with diversified and complicated landform. Therefore, the newly released, freely available and globally covered GDEM product is an alternatively promising data option and provide an important opportunity to explore LER (Li and Feng 2016; Xiao et al. 2018). However, current LER products were either challenged by coarser spatial resolution, or via the subjective selection of neighborhood

scales (Xiao et al. 2018).

An analysis of LER-based topographical SAHS for the 1 arc-second resolution GDEM products in China has not been reported to date. Appropriate LER for China was calculated and extracted at 30-m spatial resolution in this study using the optimal statistical window method. This approach can be used to systematically depict LER characteristics by analyzing their spatial distributions and correlations with population distribution. The resultant GDEM LER was then used to evaluate the topographical suitability of human settlements. The objective of this study was therefore to develop an improved evaluation model to evaluate the suitability of different terrains for sustaining human settlements, i.e., the examination of the relationship between population distribution and GDEM LER as well as their suitability. Compared with previous studies, the improvements of this study had two-fold: (1) The optimal statistical window (instead of subjective selection) was used to determine the appropriate LER over the entire country; (2) The relationship between population density and firstly-derived 30-m GDEM LER was investigated from the view of topographical suitability of human settlements in China.

1 Materials and Methods

1.1 Terrain data and pre-processing

ASTER GDEM data were used to extract terrain (or LER) features in this study. ASTER is a significantly advanced multi-spectral data source at finer spatial resolution aboard the Terra satellite launched on December 18th, 1999, and forms the basis for the GDEM version 2 (V2) that was jointly released by the U.S. National Aeronautics and Space Administration (NASA) and Japanese Ministry of Economy, Trade and Industry (METI) in 2011. These data can be freely downloaded from the NASA Land Processes Distributed Active Archive Center (LP DAAC; <https://reverb.echo.nasa.gov>) and the Earth Remote Sensing Data Analysis Center (ERSDA; <http://www.ersdac.gdem.aster.or.jp/>). GDEM encompasses the land surface between 83°N and 83°S at 1 arc second spatial resolution, covering about 99% of the total land surface area on Earth. GDEM products, divided

into 1°-by-1° tiles, were subjected to cloud masking and bad value removed (Tachikawa et al. 2011). Each tile contains at least 0.01% land area and comprises two compressed files, the DEM and quality assessment. In particular, GDEM V2 is in GeoTIFF format with geographic lat/long coordinate systems and WGS84/EGM96 geoid vertical reference system (Tachikawa et al. 2011).

GDEM V2 has been subsequently improved especially in the fields of removal of anomalous data and cloudy pixels (Tachikawa et al. 2011) and is now widely applied across a range of fields. Although it might contain outliers (e.g., both negative and higher values) at the local level, the horizontal and vertical accuracies of the global products are 30 m and 20 m at 95% confidence level, respectively (Tachikawa et al. 2011). GDEM V2 product is therefore a high-quality data source that can be used for extracting global topographical information. According to the maximum (i.e., Mount Qomolangma (8844.43 m above sea level (a.s.l.))) and minimum (i.e., Aydingkol Lake (-155 m a.s.l.)) elevations within China, anomalies (e.g. less than -155 m a.s.l.) were consistently assigned as zero (a.s.l.) while others (e.g. no data) were allocated to masked cells based using the Euclidean distance approach calculated via the Nibble tool. In addition, as we attempted to analyze the correlations between LER and population density in China, the 30 m resolution GDEM LER were resampled at a 1 km ×1 km resolution. All data pre-processing and LER-related calculation procedures were finished in ArcGIS 10.0 software.

1.2 National population data

Chinese national population density raster data for 2010 (1 km resolution) was ordered, processed, and freely downloaded from the National Earth System Science Data Sharing Infrastructure, National Science and Technology Infrastructure of China (<http://www.geodata.cn>). In particular, the 1 km ×1 km grid population data products were generated on the basis of digital elevation, net primary productivity, city size and density, and traffic infrastructure density data sets (Liu et al. 2003). Thus, after transformation into the same projection with that of ASTER GDEM, national-level data were used to detect the relationship between terrain (i.e., LER) and

Table 1 Local elevation range (LER) for different neighborhood windows in China.

No.	Window	Grid area (km ²)	Maximum LER (m)	Average LER (m)	No.	Window	Grid area (km ²)	Maximum LER (m)	Average LER (m)
1	2 × 2	0.0036	6275	1528.7	48	49 × 49	2.1609	6745	3249.6
2	3 × 3	0.0081	6291	2016.3	49	50 × 50	2.2500	6745	3256.7
3	4 × 4	0.0144	6313	2249.7	50	51 × 51	2.3409	6750	3261.7
...
19	20 × 20	0.3600	6645	3057.5	99	100 × 100	9.0000	6983	3432.3
...
46	47 × 47	1.9881	6745	3241.0	198	199 × 199	35.6409	7303	3580.1
47	48 × 48	2.0736	6745	3245.9	199	200 × 200	36.0000	7303	3580.6

population distribution. In particular, the topographical SAHS refers to the relationship between population distribution and LER (or terrain) as well as their suitability degree of population distribution.

1.3 Extraction method of local elevation range (LER)

The characteristics of LER synthetically reflect the incision depth and altitude gradient of certain region and reveal variations in regional topography. Because our previous researches have shown that terrain relief (or LER) can be effectively used to evaluate human settlements (Feng et al. 2009, 2010; Xiao et al. 2018), we continued to utilize the elevation range but incorporated more neighborhoods (potential statistical windows) and finer-scale spatial resolution (30 m) in order to improve the accuracy of results by determining the optimal LER calculating window. Thus, GDEM LER in China was extracted using the window analysis method and the Focal Statistics function (Batch module) for different neighborhood windows (Rectangle, 2 × 2, 3 × 3,, 200 × 200; 199 in total) each with a step length of one (see Table 1). This grade-level window analysis greatly contributes to determining LER thresholds and improves our terrain evaluation results compared with previous studies due to subjective selection of calculating window (Feng et al. 2007, 2008, 2009, 2010).

As shown in Table 1, the average values of LER increase rapidly in accordance with increment of step length in China. Exploratory analysis also revealed the presence of a logarithmic relationship between grid units and corresponding average LER, with the R² value of 0.98 (Figure 1). Figure 1 also shows a relatively stable distribution for LER growth rate that increases slowly when the area of

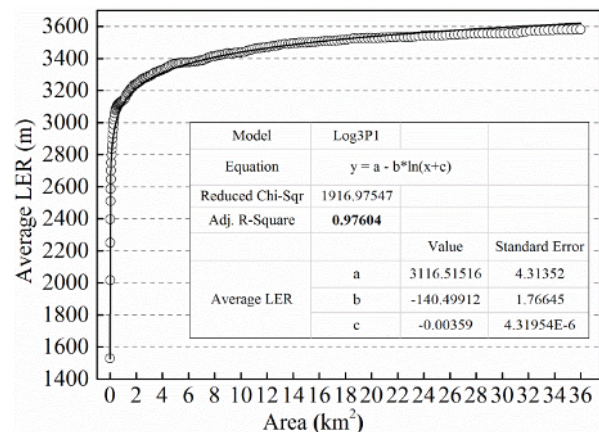


Figure 1 Fitted curve for the relationship between different grid units and local elevation range (LER) in China.

grid units reaches a specific threshold value. This implies that there is a threshold inflection point value at a certain grid unit which can be determined using change point analysis, although visually determining this level was problematic (Wang et al. 2016). Recent studies have shown that the determination of the appropriate statistical unit is key to extract appropriate LER (Yu et al. 2015; Wang et al. 2016; Xiao et al. 2018). It is noteworthy that the mean change point method has been applied in several recent studies to calculate the appropriate statistical window for determining regional LER with DEM data in China (Chen et al. 2013; Wang et al. 2016) and MSEA (Xiao et al. 2018). For more information about the calculating process of appropriate LER using mean change point method, one can refer to our previous study (Xiao et al. 2018).

1.4 Evaluating the topographical suitability of human settlements

We have finished the 1 km × 1 km grid size assessment studies of suitability of human

settlements in China, including terrain, climate, hydrology, vegetation coverage and land use (Feng et al. 2008, 2010). In the previous studies, the authors developed a multi-factor integrated evaluation model with five geographic elements (i.e., terrain, climate, hydrology, vegetation and land use) to distinguish the individual relative effects on human settlements. The individual correlation coefficients with population distribution were re-used to assess the comprehensive effects on human settlements (Feng et al. 2009, 2010). In this study, two improvements (i.e., more neighborhoods and optimal statistical windows at a finer spatial resolution (30 m)) are made to evaluate the suitability of different terrains for sustaining human settlements via the application of appropriate LER. Differed from the previous studies that used the relief degree of land surface by multiplying a 500-m mountain to assess the topographical suitability of human settlements (or population distribution) using a 25 km² window at 1 km grid cell, we attempted to do the same assessment with LER within the optimal window size of 2.34 km² at 30 m grid cell.

2 Results

2.1 Optimal statistical window for calculating appropriate LER

As discussed, one important prerequisite for the mean change point method is the determination of the unique peak value (i.e., the inflection point) (Chen 1988). An optimal window was determined using above-mentioned mean change point method in order to calculate the appropriate LER. Figure 2 shows that the difference values (i.e., between S and S_i) increase rapidly prior to an inflection or change point, but then significantly decrease, showing a unimodal distribution or an inverted U-shape. For more information about the S and S_i , one can refer to our previous study (Xiao et al. 2018). This scatter plot also shows that values for differences reached a maximum at the 50th point (the red square in Figure 2), or an optimal statistical grid window of 51 × 51, approximately equal to 2.34 km² area (Table 1). These results show that the mean change point method can be applied to detect the most

appropriate grid window size for further analysis. Appropriate GDEM LER was therefore used to evaluate the topographical suitability of human settlements in China.

2.2 Spatial characteristics of LER

Figure 3 illustrates the spatial distribution of national LER within a 51 × 51 grid window, showing the LER values within China ranging between zero and 6750 m (with an average of 250.57 m). Specifically, the accumulative frequency is 63.15% when the LER value is 250 m, and 85.22% in case of 500 m of LER. It clearly indicates that

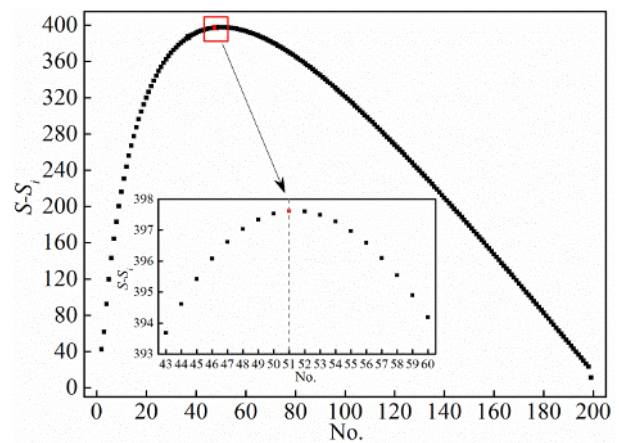


Figure 2 Scatter diagram to show the change in difference values between S and S_i using the change point method in China. The red square in this figure marks the occurrence of the inflection point (i.e., the optimal statistical window).

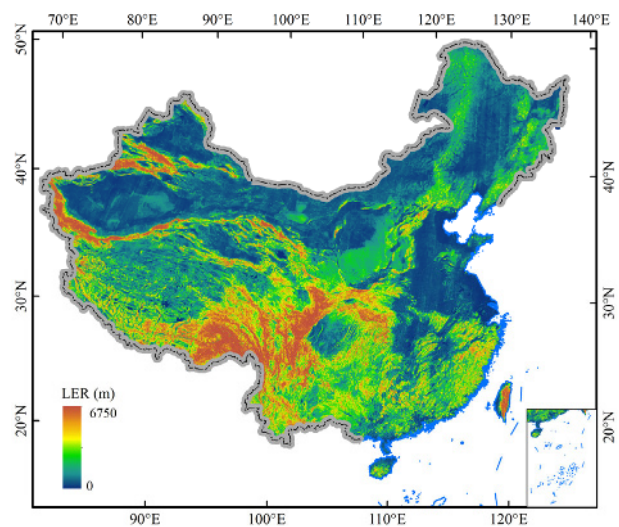


Figure 3 Local elevation range (LER) of China using an optimal statistical window (i.e., a 51×51 unit grid).

there was a significantly low elevation range in most of China. Spatially, LER value in southern and western China tend to be greater than their counterparts in the north and east (Figure 3), although with larger values in the Hengduan Mountains, Tianshan Mountains, and Qinling Mountains and southeastern Tibetan Plateau (TP). Smaller LER values are seen in the Northeastern China Plain, Tarim Basin, Inner Mongolian Plateau, and North China Plain, as well as in the Sichuan Basin, Poyang Lake Plain and Dongting Lake Plain. Results also show that the low LER also distributed in the delta areas of the Yellow River, Yangtze River, Pearl River, and Liaohe River (Figure 3). We further analyzed and investigated the spatial variations in LER values at different latitudes and longitudes in the next section.

2.2.1 Latitudinal variations

We explored the spatial distribution of LER based on the variations in various latitudes (i.e., 25°N, 30°N, 35°N, and 40°N) (Figure 4) and longitudes (i.e., 85°E, 95°E, 105°E, and 115°E) (Figure 5) in China. Figure 4 shows the changes in LER values greatly varied with latitudes in China. Results show that the average LER curves along latitude exhibit a saddle-shape and decrease overall as longitude increases. Terrain characteristics of more mountains in the north and flatter area in the east within China might well explain this trend. Specially, there is an obvious valley-shape in LER data between 78°E and 93°E due to the Tarim Basin and Junggar Basin and an apex between 93°E and 103°E because of the Qilian Mountains and Hengduan Mountains. It further decreases because of the presence of additional plains and deltas (e.g., the Northeastern China Plain, North China Plain, and middle and lower reaches of the Yangtze River Plain).

Figure 4 illustrate characteristics of the LER at five degree intervals, namely the latitudes of 25°N, 30°N, 35°N, and 40°N. Figure 4 also reveals the LER dynamics at a latitude of 25°N ranging between zero and 1300 m. Along a transect from west to east, the LER fluctuates significantly in the Hengduan Mountains, decreases on the Yunnan-Guizhou Plateau, and increases again in the southwestern Guizhou Mountains before markedly decreasing in the Guangxi Basin and increasing within the Jiangnan Hilly Region. Similarly, at

30°N, the LER fluctuates sharply along the Himalayas and decrease towards the margins of these mountains and TP before notably decreasing within the Yarlung Zangbo Grand Canyon, decreasing again within the Sichuan Basin and middle and lower reaches of the Yangtze River Plain, and increasing within the North Jiangnan Hilly Region. The LER at 35°N fluctuates sharply along a transect between 78°E and 83°E because of the Kunlun Mountains and then decreases on the TP, Loess Plateau, and North China Plain, before increasing again within the Yimeng Mountain Areas in Shandong Province. Finally, the LER at 40°N only slightly fluctuates because of the Tarim Basin, Inner Mongolian Plateau, and North China Plain. In addition, the LER of 40°N remains relatively low in these regions, typically lower than 400 m.

Figure 5 illustrates the changes in LER with

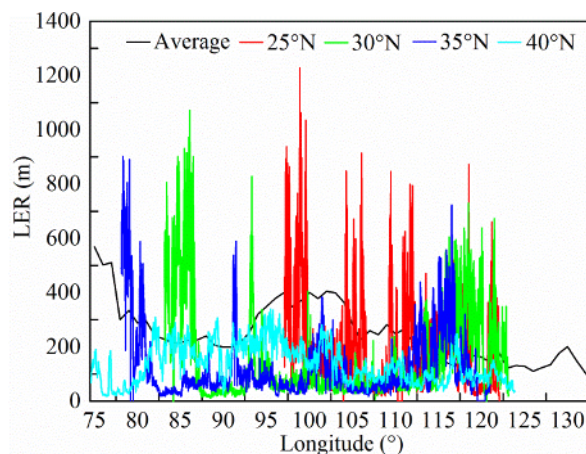


Figure 4 Changes in the local elevation range (LER) with different latitudes in China.

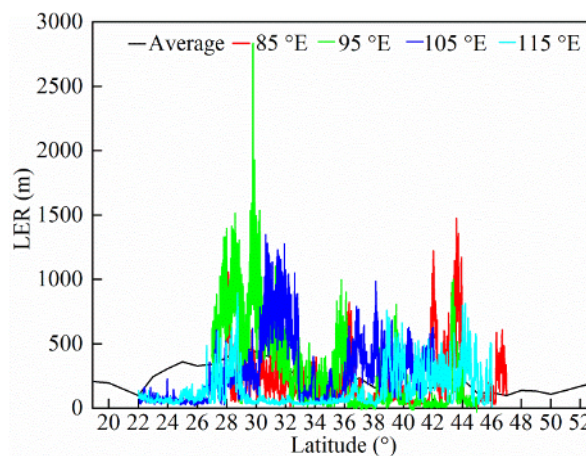


Figure 5 Changes in the local elevation range (LER) with different longitudes in China.

different longitudes in China. Results show that LER of China generally decreases as latitude increases, in accordance with the geomorphic characteristics. For example, more plains (e.g., the North China Plain) and plateaus (e.g., the Inner Mongolian Plateau) present in the north of China, while there are more mountains (e.g., the Himalayas) and hills (e.g., the Jiangnan Hilly Region) in the south. Figure 5 reveals the presence of a valley-shape at about 22°N due to the Guangdong and Guangxi Hills, with their LER much lower than those within the Himalayas and Hengduan Mountains between 22°N and 32°N. The LER also gradually decreases in the areas to the north of 32°N because of the North China Plain, Loess Plateau, Tarim Basin, Inner Mongolian Plateau, and northeastern China Plain.

Figure 5 illustrate changes in LER at ten degree intervals of longitude, i.e., 85°E, 95°E, 105°E, and 115°E. At 85°E, the LER fluctuates on the TP and increases to 1,000 m around 37°N (the edge of the TP) before decreasing markedly within the Tarim Basin, increasing again in the Tianshan Mountains, and further decreasing within the Junggar Basin. Figure 5 shows that the LER fluctuates sharply at a longitude of 95°E, displaying an apex-shape at about 30°N due to the Yarlung Zangbo Grand Canyon, while LER at 105°E fluctuate sharply between 30°N and 33°N because of the boundaries between the Sichuan Basin and Loess Plateau. These values then decrease notably on the Loess Plateau and fluctuate again at the

Inner Mongolian Plateau. In contrast, at 115°E, LER fluctuates within the Jiangnan Hilly Region (between 27°N and 29°N), decreases markedly within the middle and lower reaches of the Yangtze River Plain and North China Plain between 29°N and 39°N, and increases again at the margin of the Inner Mongolian Plateau.

2.3 Correlation between LER and population density

Among the above-mentioned five geographic factors influencing human habitat, two of them (terrain and climate) are dominant and determinative (Feng et al. 2009). Currently, we only focused on the topographical SAHS due to the accessibility of GDEM data of global coverage. In order to re-evaluate the suitability of different terrains suitability for sustaining human settlements in China, the 30-m GDEM LER were resampled to 1 km × 1 km grid cell, the same spatial resolution with the 2010 national population density data. Figure 6 illustrates the relationship between LER and population density. The relationship between the two variables was highly correlated with the R² value of 0.81 (Figure 6b), implying that LER exerts an important and positive influence on Chinese population distribution.

Statistics at different LER grades revealed that the Chinese population in 2010 was mostly located within low-range elevation regions (Figure 6b), which is consistent with our previous research

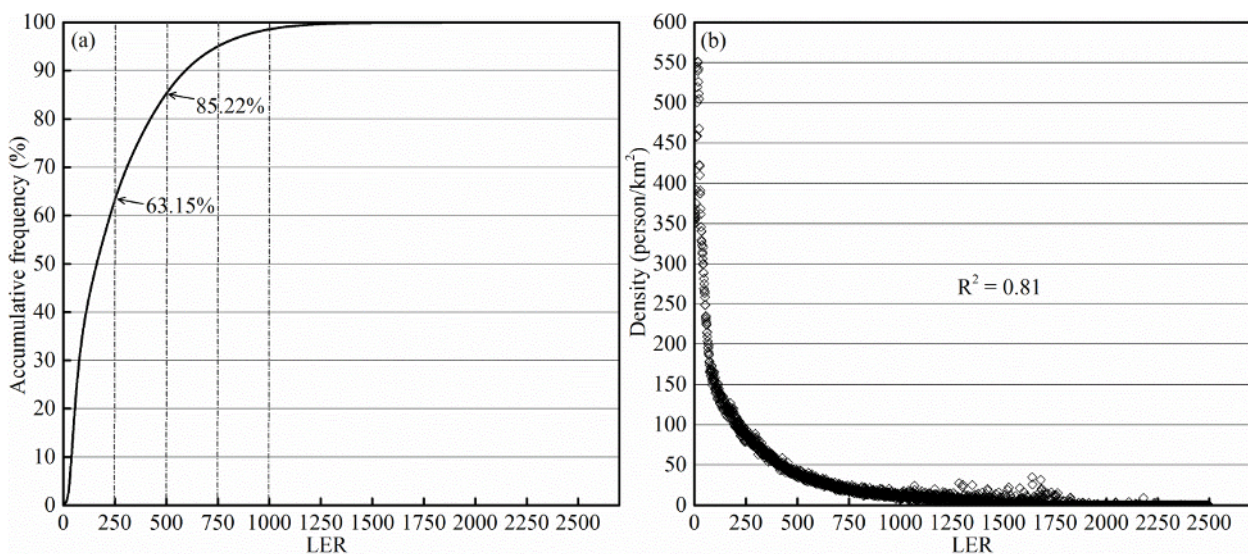


Figure 6 Correlations between local elevation range (LER) and accumulative population (a) frequency and (b) density.

(Feng et al. 2007, 2008). It shows that the accumulative level of population density was 37.27% when the LER is 100 m, followed by the proportions of 63.15% and 85.22% in the cases of LER less than 250 m and 500 m, respectively (Figure 6). However, the relevant population ratio was merely 1.45% when the LER range is greater than 1000 m. These results demonstrated once again that terrain significantly influences the population distribution within China and should be considered as an important parameter when evaluating the topographical suitability of human settlements.

2.4 Analysis of the topographical SAHS

With 1 km grid data of population density, GDEM LER, and the results of our previous work (Feng et al. 2009, 2010), five distinct levels of terrain suitability for human settlements were determined, i.e., the non-suitable area (NSA), critical suitable area (CSA), low suitable area (LSA), moderate suitable area (MSA), and high suitable area (HSA). The suitability of different terrains for sustaining human settlements within China based on LER is illustrated in Figure 7. Results show that the spatial distribution of the topographical SAHS decreases from the southeastern coastal zone of the

Table 2 The land area and population in the five regions with different terrains suitability for sustaining human settlements in China.

Suitability types of human settlements	Land area		Population	
	Area ($\times 10^4$ km ²)	Proportion (%)	Number (million)	Proportion (%)
Non-suitable area (NSA)	60.29	6.28	2.31	0.17
Critical suitable area (CSA)	236.16	24.60	13.27	0.99
Low suitable area (LSA)	239.71	24.97	142.99	10.67
Moderate suitable area (MSA)	273.89	28.53	369.29	27.55
High suitable area (HSA)	149.95	15.62	812.53	60.62

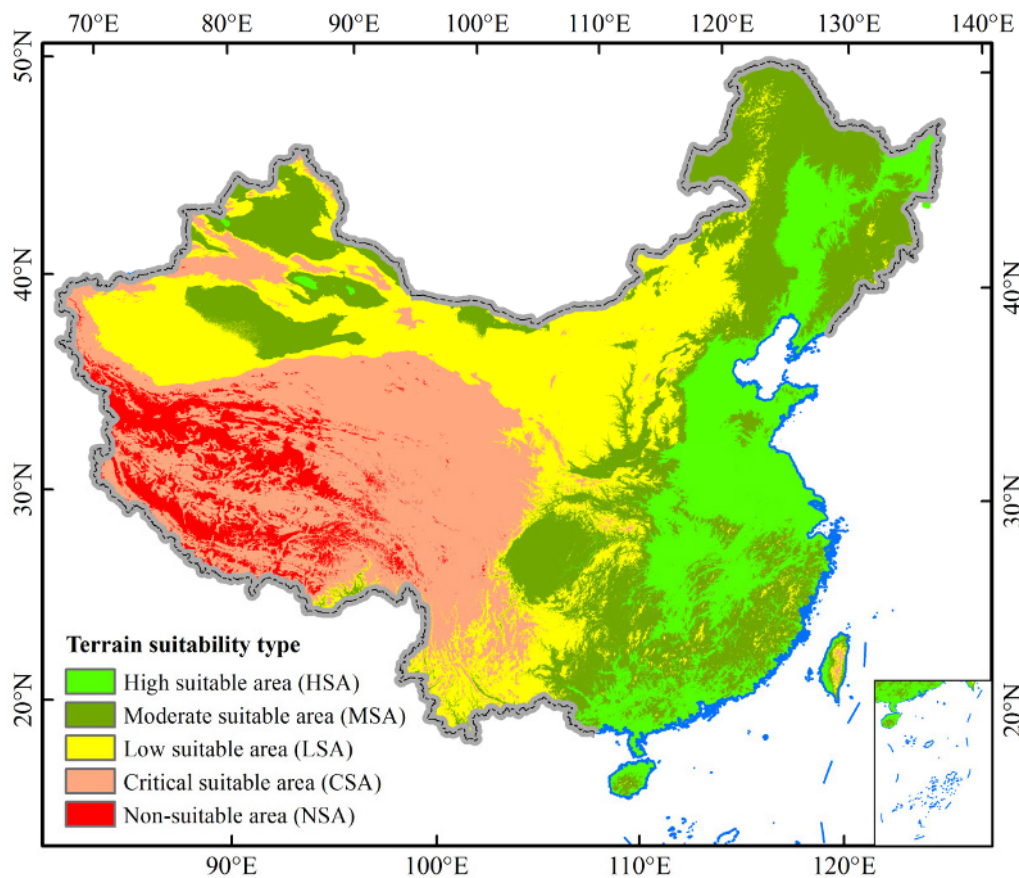


Figure 7 Distribution of different terrains for sustaining human settlements in China.

country into northwestern inland areas, as plains and basins transition to plateaus and mountains.

The evaluation results (Figure 7, Table 2) showed that: (1) the NSA, encompassed a small population of 2.31 million (only 0.17% of the total) within China, covering an area of 60.29×10^4 km² (6.28% of the total), which are mainly distributed in the TP, Hengduan Mountains, and parts of the Qilian Mountains. (2) The CSA, had a population of 13.27 million (0.99% of the total), with an area of 236.16×10^4 km² (24.60% of the total), mainly distributed within the hinterland of the TP, Tianshan Mountains, Qilian Mountains, Kunlun Mountains, Hengduan Mountains, and western regions of the Yunnan-Guizhou Plateau. (3) A population of 142.99 million (10.67% of the total) resided in the LSA, holding an area of 239.71×10^4 km² (24.97% of the total), primarily located in the Loess Plateau, west of the Inner Mongolian Plateau, southwestern Tarim Basin, Junggar Basin, periphery of the Sichuan Basin, central part of the Yunnan-Guizhou Plateau, parts of the Jiangnan Hilly Region, and the river valleys of southern Tibet. (4) The second largest population of 369.29 million (27.55% of the total) lived in the MSA, covering an area of 273.89×10^4 km² (28.53% of the total), normally in the Sichuan Basin, southeast of the Yunnan-Guizhou Plateau, Nanling Mountains, northeastern Tarim Basin, and the Da (Greater) and Xiao (Lesser) Hinggan Mountains. (5) The HSA, with an area of 149.95×10^4 km² (15.62% of the total), were crowded by the largest population of 812.53 million (60.62% of the total) in the flat plains, such as the Northeastern China Plain, North China Plain, middle and lower reaches of the Yangtze River Plain, and southeastern coast of China.

3 Discussion

This study calculated the LER-based optimal statistical window method based on the mean change point approach. Our aims were to delineate the spatial features of GDEM LER within China and explore its relationship with gridded population density in 2010. It enabled us to evaluate the national topographical SAHS from two aspects. First, and most importantly, compared with the subjective selection of neighborhood

scales, the mean change point method was more objective in calculating LER. The second aspect is that the 30 m GDEM LER calculated based on the optimal window (or an area of 2.34 km²) used in this study greatly contribute to understanding the regional details of Chinese terrain. That said, the topographical SAHS with 30 m GDEM appropriate LER is viewed as a developed version in the two mentioned aspects (Feng et al. 2007, 2008, 2009, 2010; Wang et al. 2016). More importantly, the appropriate LER analyses in China (i.e., a 51×51 unit grid) and MSEA (i.e., a 38×38 unit grid) (Xiao et al. 2018) clearly indicated that the optimum window size for calculating regional LER is dynamic but unique.

The 30-m GDEM LER provides an important baseline database for further topographic SAHS and its correlations with the gridded population distribution at larger scale. However, the data quality of GDEM may affect the appropriate LER derived from the mean change point method. Actually, GDEM is subject to elevation error, root-mean-square error (RMSE), and cloud contamination, although the topographic features are sharper in GDEM V2 compared with GDEM V1 (Li et al. 2013; Tachikawa et al. 2011). In particular, the standard deviation and RMSE of elevation error for GDEM V2 are high in forest-covered regions and low in open areas, e.g., water body and farmlands. Thus, for extracting LER, extensive pre-processing procedures including cloud and bad value removal are also needed. Despite some flaws, this study indicates that GDEM data provides useful information on terrain analysis and its suitability of different terrains for sustaining human settlements. On this basis, further analyses that incorporate additional factors (e.g., climate and hydrology) will be required for comprehensive evaluation of human settlements suitability.

4 Conclusions

The appropriate LER map for China was firstly extracted in this study by utilizing ASTER GDEM at a 1 arc second (approximately 30-m) spatial resolution with the optimal statistical window approach (i.e., the mean change point method). The systematic characteristics of LER were also evaluated via ratio structure analysis, spatial

distributions, and correlations with population distribution. It enabled us to evaluate the topographical SAHS in China. Our conclusions are as follows:

(1) The optimal statistical window for calculating Chinese GDEM-based LER was a 51×51 grid unit (width \times height) within a rectangular neighborhood, corresponding to an area of about 2.34 km². Results show that 30-m appropriate GDEM LER is significantly related to the spatial distribution features of landforms in China. Our study again demonstrated the great potential of the mean change point method for determining an optimal statistical window.

(2) The majority (85.22%) of LER in China are smaller than 500 m. Spatially, the LER values in the southern and western China were greater than their counterparts in the north and east. The LER values also decrease as latitudes and longitudes increase, showing a declining trend from southwest to northeast. As a whole, the variations of LER at latitudes of 25°N, 30°N, 35°N, and 40°N, as well as at longitudes of 85°E, 95°E, 105°E, and 115°E were able to reflect the major terrain characteristics within the country.

(3) The relationship between LER and population density was highly correlated in 2010 (i.e., the R² value of 0.81). It showed that 85.22% of the Chinese population is located within the regions where the LER is lower than 500 m. It

shows that LER have significantly impacted the national population distribution and should be seriously considered as one of the important factors when evaluating the topographical suitability of human settlements.

(4) The spatial distribution of different terrains that is suitable for human settlements in China decreases from the southeastern coastal zone with plains and basins into the northwestern inland areas of plateaus and mountains. The total area of moderate to high suitable level was 423.84×10^4 km², accounting for about 44.15% of China, with 88.17% of the national population crowded within these zones.

Acknowledgements

The study was supported by the National Key Research and Development Program (Grand No. 2016YFC0503506) and the National Natural Science Foundation of China (Grand No. 41430861). The authors thank for the population data support from “National Earth System Science Data Sharing Infrastructure, National Science & Technology Infrastructure of China. (<http://www.geodata.cn>)”. We also specially thank the editors and anonymous reviewers for their comments that helped to improve this manuscript.

References

- Chen L, Zhang WZ, Yang YZ, et al. (2013) Disparities in residential environment and satisfaction among urban residents in Dalian, China. *Habitat International* 40: 100-108. <https://doi.org/10.1016/j.habitatint.2013.03.002>
- Chen X (1988) Inference in a simple change point model. *Scientia Sinica (A)* 8: 654-667.
- Chen XX, Chang Q, Guo B, et al. (2013) Analytical study of the relief amplitude in China based on SRTM DEM data. *Journal of Basic Science and Engineering* 21(4): 670-678. (In Chinese) <https://doi.org/10.3969/j.issn.1005-0930.2013.04.009>
- Chiang CL, Liang JJ (2013) An evaluation approach for livable urban environments. *Environment Science and Pollution Research* 20(8): 5229-5242. <https://doi.org/10.1007/s11356-013-1511-6>
- Doxiadis CA (1975) *Action for Human Settlements*. Athens Publishing, Center Athens.
- Emmanuel R (2005) Thermal comfort implications of urbanization in a warm-humid city: The Colombo Metropolitan Region (CMR), Sri Lanka. *Building and Environment* 40(12): 1591-1601. <https://doi.org/10.1016/j.buildenv.2004.12.004>
- Esch T, Marconcini M, Marmanis D, et al. (2014) Dimensioning urbanization-An advanced procedure for characterizing human settlement properties and patterns using spatial network analysis. *Applied Geography* 55: 212-228. <https://doi.org/10.1016/j.apgeog.2014.09.009>
- Fang YP, Yang B (2016) Spatial distribution of mountainous regions and classification of economic development in China. *Journal of Mountain Science* 13(6): 1120-1138. <https://doi.org/10.1007/s11629-015-3714-4>
- Feng Z M, Tang Y, Yang YZ, et al. (2007) The relief degree of land surface in China and its correlation with population distribution. *Acta Geographica Sinica* 62(10): 1073-1082. (In Chinese)
- Feng ZM, Tang Y, Yang YZ, et al. (2008) Relief degree of land surface and its influence on population distribution in China. *Journal of Geographical Sciences* 18(2): 237-246. <https://doi.org/10.1007/s11442-008-0237-8>
- Feng ZM, Yang YZ, Zhang D, et al. (2009) Natural environment suitability for human settlements in China based on GIS. *Journal of Geographical Sciences* 19(2): 437-446. <https://doi.org/10.1007/s11442-009-0437-x>
- Feng ZM, Yang YZ, You Z, et al. (2010) A GIS-based study on sustainable human settlements functional division in China. *Journal of Resources and Ecology* 1(4): 331-338. <https://doi.org/10.3969/j.issn.1674-764x.2010.04.005>

- Kotus J, Rzeszewski M (2013) Between disorder and livability: Case of one street in post-socialist city. *Cities* 32(4): 123-134. <https://doi.org/10.1016/j.cities.2013.03.015>
- Li P, Shi C, Li Z, et al. (2013) Evaluation of ASTER GDEM using GPS benchmarks and SRTM in China. *International Journal of Remote Sensing* 34(5): 1744-1771. <https://doi.org/10.1016/j.jag.2016.05.008>
- Li YC, Liu CX, Zhang H, et al. (2011) Evaluation on the human settlements environment suitability in the three Gorges reservoir area of Chongqing based on RS and GIS. *Journal of Geographical Sciences* 21(2): 346-358. <https://doi.org/10.1007/s11442-011-0849-2>
- Liu Y, Deng W, Song XQ (2015) Relief degree of land surface and population distribution of mountainous areas in China. *Journal of Mountain Science* 12(2): 518-532. <https://doi.org/10.1007/s11629-013-2937-5>
- Liu JY, Yue TX, Wang YA, et al. (2003) Digital simulation of population density in China. *Acta Geographica Sinica* 58(1): 1724. (In Chinese)
- Ma RF, Wang TF, Zhang W, et al. (2016) Overview and progress of Chinese geographical human settlement research. *Journal of Geographical Sciences* 26(8): 1159-1175. <https://doi.org/10.1007/s11442-016-1320-1>
- Meybeck M, Green P, Vörösmarty C (2001) A new typology for mountains and other relief classes. *Mountain Research Development* 21(1): 34-45. [https://doi.org/10.1659/0276-4741\(2001\)021\[0034:ANTFMA\]2.0.CO;2](https://doi.org/10.1659/0276-4741(2001)021[0034:ANTFMA]2.0.CO;2)
- Podobnikar T (2012) Detecting Mountain Peaks and Delineating Their Shapes Using Digital Elevation Models, Remote Sensing and Geographic Information Systems Using Autometric Methodological Procedures. *Remote Sensing* 4(3): 784-809. <https://doi.org/10.3390/rs4030784>
- Richard M, Walter F, John M, et al. (2008) Practical appraisal of sustainable development: Methodologies for sustainability measurement at settlement level. *Environmental Impact Assessment Review* 28: 144-165. <https://doi.org/10.1016/j.eiar.2007.06.003>
- Rodríguez E, Morris CS, Belz JE (2006) A global assessment of the SRTM performance. *Photogrammetric Engineering and Remote Sensing* 72(3): 249-60. <https://doi.org/10.14358/PERS.72.3.249>
- Satgé F, Bonnet MP, Timouk F, et al. (2015) Accuracy assessment of SRTM v4 and ASTER GDEM v2 over the Altiplano watershed using ICESat/GLAS data. *International Journal of Remote Sensing* 36 (2): 465-488. <https://doi.org/10.1080/01431161.2014.999166>
- Tachikawa T, Hato M, Kaku M, et al. (2011) The characteristics of ASTER GDEM version 2. *IEEE International Geoscience and Remote Sensing Symposium, IGARSS 2011, Vancouver, BC*. <https://doi.org/10.1109/IGARSS.2011.6050017>
- Taubenböck H, Esch T, Felbier A, et al. (2012) Monitoring urbanization in mega cities from space. *Remote Sensing of Environment*, 117: 162-176. <https://doi.org/10.1016/j.rse.2011.09.015>
- Tritsch I, Le Tourneau F (2016) Population densities and deforestation in the Brazilian Amazon: New insights on the current human settlement patterns. *Applied Geography* 76: 163-172. <https://doi.org/10.1016/j.apgeog.2016.09.022>
- Tu HM, Liu ZD (1991) Study on relief amplitude in China. *Acta Geodaetica et Cartographica Sinica* 20(4): 311-319. (In Chinese)
- USGS (1996) Global 30 Arc-Second Elevation (GTOPO30). Available online: <https://lta.cr.usgs.gov/GTOPO30>, accessed on 27 October 2017.
- USGS (2010) Global Multi-resolution Terrain Elevation Data 2010 (GMTED2010). Available online: <https://lta.cr.usgs.gov/GMTED2010>, accessed on 27 October 2017.
- Wang RH, Zhang W, Pu L, et al. (2016) Analysis on the relief amplitude in Northeast China based on ASTER GDEM and mean change point method. *Journal of Arid Land Resources and Environment* 30(6): 49-54. (In Chinese) <https://doi.org/10.13448/j.cnki.jalre.2016.180>
- Wang Y, Jin C, Lu MQ, et al. (2017) Assessing the suitability of regional human settlements environment from a different preferences perspective: A case study of Zhejiang Province, China. *Habitat International* 70: 1-12. <https://doi.org/10.1016/j.habitatint.2017.09.010>
- Wei W, Shi PJ, Zhou JJ, et al. (2013) Environmental suitability evaluation for human settlements in an arid inland river basin: A case study of the Shiyang river basin. *Journal of Geographical Sciences* 23(2): 331-343. <https://doi.org/10.1007/s11442-013-1013-y>
- Wu CD, Lung SC, Jan JF (2013) Development of a 3-D urbanization index using digital terrain models for surface urban heat island effects. *ISPRS Journal of Photogrammetry and Remote Sensing* 81(7): 1-11. <https://doi.org/10.1016/j.isprsjprs.2013.03.009>
- Wu LY (2001) Introduction to Sciences of Human Settlements. Beijing: China Architecture and Building Press.
- Xiao CW, Li P, Feng ZM (2018) Re-delineating mountainous regions with three topographic parameters in Mainland Southeast Asia using ASTER GDEM. *Journal of Mountain Science* 15(8): 1728-1740. <https://doi.org/10.1007/s11629-017-4746-8>
- Yang X, Zhang WZ (2016) Combining natural and human elements to evaluate regional human settlements quality based on raster data: A case study in Beijing-Tianjin-Hebei region. *Acta Geographica Sinica* 71(12): 2141-2154. (In Chinese) <https://doi.org/10.11821/dlxb201612006>
- Yang LP, Meng XM, Zhang XQ (2011) SRTM DEM and its application advances. *International Journal of Remote Sensing* 32 (14): 3875-3896. <https://doi.org/10.1080/01431161003786016>
- Yue LW, Shen H, Zhang L, et al. (2017) High-quality seamless DEM generation blending SRTM-1, ASTER GDEM v2 and ICESat/GLAS observations. *ISPRS Journal of Photogrammetry and Remote Sensing* 123:20-34. <https://doi.org/10.1016/j.isprsjprs.2016.11.002>
- Zhang Q, Zhu C, Liu C, et al. (2005) Environmental change and its impacts on human settlement in the Yangtze Delta, P.R. China. *Catena* 60(3): 267-277. <https://doi.org/10.1016/j.catena.2013.10.012>
- Zhong XH, Liu SZ (2014) Research on the Mountain Classification in China. *Mountain Research* 32(2): 129-140. (In Chinese) <https://doi.org/10.16089/j.cnki.1008-2786.2014.02.006>
- Zhu JS, Tian SF, Tan K, et al. (2016) Human settlement analysis based on multitemporal remote sensing data: A case study of Xuzhou city, China. *Chinese Geographical Science* 26(3): 389-400. <https://doi.org/10.1007/s11769-016-0815-0>

Reproduced with permission of copyright owner. Further reproduction prohibited without permission.